

# VALIDATING UNCERTAINTY IN MEDICAL IMAGE TRANSLATION

Jacob C. Reinhold\*, Yufan He\*, Shizhong Han<sup>†</sup>, Yunqiang Chen<sup>†</sup>, Dashan Gao<sup>†</sup>,  
Junghoon Lee<sup>‡</sup>, Jerry L. Prince<sup>\*◦</sup>, IEEE Fellow, Aaron Carass<sup>\*◦</sup>, IEEE Member

\* Department of Electrical and Computer Engineering, Johns Hopkins University, Baltimore, MD, USA

<sup>†</sup> 12 Sigma Technologies, San Diego, CA USA

<sup>‡</sup> Department of Radiation Oncology, Johns Hopkins School of Medicine, Baltimore, MD, USA

<sup>◦</sup> Department of Computer Science, Johns Hopkins University, Baltimore, MD, USA

## ABSTRACT

Medical images are increasingly used as input to deep neural networks to produce quantitative values that aid researchers and clinicians. However, standard deep neural networks do not provide a reliable measure of uncertainty in those quantitative values. Recent work has shown that using dropout during training and testing can provide estimates of uncertainty. In this work, we investigate using dropout to estimate epistemic and aleatoric uncertainty in a CT-to-MR image translation task. We show that both types of uncertainty are captured, as defined, providing confidence in the output uncertainty estimates.

**Index Terms**— Image translation, uncertainty estimation.

## 1. INTRODUCTION

We build on recent developments for estimating uncertainty in deep neural networks (DNNs) to give granular estimates of uncertainty in image translation tasks. We validate that estimates of uncertainty are captured, as defined, and show that uncertainty estimates can inform users about what the model knows and does not know, as well as provide insight into limitations inherent in the data and model.

Estimating uncertainty in DNNs is important since DNNs are, generally, poorly calibrated [1]. Calibration in this context refers to the average confidence in prediction diverging from model accuracy; in the case of DNNs, the models are usually overconfident which is potentially unsafe. Estimating uncertainty does not intrinsically calibrate a DNN, but uncertainty—in conjunction with other measurements of model accuracy—can improve user’s trust of neural network results.

Uncertainty has two main subtypes: *epistemic* and *aleatoric* [2]. Epistemic uncertainty corresponds to a model’s ignorance and aleatoric uncertainty is related to the intrinsic variance in the data. We want to capture these two types of uncertainty in a medical image translation task (sometimes called image synthesis). Medical image translation consists of learning a function to transform image intensities between either two magnetic resonance (MR) contrasts or two image

modalities, such as  $T_1$ -weighted ( $T_1$ -w) MR and computed tomography (CT)—the task we explore in this paper.

We want to estimate these two granular types of uncertainty because 1) epistemic uncertainty shows what kind of additional training data needs to be acquired for optimal performance and highlights anomalies present in the data and 2) aleatoric uncertainty shows inherent limitations of the collected data. Furthermore, capturing one type of uncertainty but not the other is insufficient to estimate the *predictive* uncertainty—an encompassing measure which describes how well any voxel can be predicted. Uncertainty estimation in image translation, segmentation, and super-resolution has been explored [3, 4, 5]; however, in this work, we verify that the epistemic and aleatoric uncertainty estimates captured in an image translation task align with the definitions of the terms.

To estimate uncertainty, we use the work of Gal and Ghahramani [6], who show that dropout [7] can be used to learn a variational distribution over the weights of a DNN—a form of approximate Bayesian inference. Then, in deployment, dropout is used in a Monte Carlo fashion to draw weights from this fitted variational distribution. The sample variance of the output from several stochastic forward passes corresponds to epistemic uncertainty. Aleatoric uncertainty is captured by modifying the network architecture to create an additional output that corresponds to a variance parameter, which is fit by changing the loss function [8]. We do this by modifying a state-of-the-art supervised image translation DNN—a U-Net [9]—to capture the two primary types of uncertainty.

## 2. METHODS

In this section, we describe 1) the relevant uncertainty estimation theory and 2) our modifications to a U-Net to estimate uncertainty.

### 2.1. Uncertainty estimation

We wish to estimate predictive uncertainty and we use the variance of the prediction as a proxy. Predictive uncertainty

can be split into two parts which separately estimate epistemic and aleatoric uncertainty.

We refer the reader to Kendall and Gal [8] for a full derivation of the loss function and predictive variance. See Reinhold et al. [10] for additional context to our specific method. Briefly, for paired (flattened) training data  $\mathbf{x}, \mathbf{y} \in \mathbb{R}^M$ , our loss function will be:

$$\mathcal{L}(\mathbf{y}, \hat{\mathbf{y}}) = \frac{1}{M} \sum_{i=1}^M \frac{1}{2} \hat{\sigma}_i^{-2} \|\mathbf{y}_i - \hat{\mathbf{y}}_i\|_2^2 + \frac{1}{2} \log \hat{\sigma}_i^2, \quad (1)$$

where  $\hat{\mathbf{y}} = f_{\hat{\mathbf{y}}}^{\mathbf{W}}(\mathbf{x})$  and  $\hat{\sigma}^2 = f_{\hat{\sigma}^2}^{\mathbf{W}}(\mathbf{x})$  are each outputs of a multi-task neural network  $f^{\mathbf{W}}(\cdot)$ . When we learn the weights,  $\mathbf{W}$ , according to Eq. (1), we are doing maximum likelihood estimation not only for  $\hat{\mathbf{y}}$ , but for the parameter  $\hat{\sigma}^2$ , which is a per-voxel estimate of the data variance—a quantity related to aleatoric uncertainty.

The predictive variance of a test sample  $\mathbf{x}^*$ , with unseen target  $\mathbf{y}^*$ , can be approximated as follows:

$$\text{Var}(\mathbf{y}^*) \approx \underbrace{\frac{1}{T} \sum_{t=1}^T \text{diag}(\hat{\sigma}_{(t)}^2)}_{\text{aleatoric}} + \underbrace{\frac{1}{T} \sum_{t=1}^T \hat{\mathbf{y}}_{(t)}^2 - \left( \frac{1}{T} \sum_{t=1}^T \hat{\mathbf{y}}_{(t)} \right)^2}_{\text{epistemic}},$$

where  $T$  is the number of sampled weights (sampled with dropout at test time). Consequently, the epistemic uncertainty is the term in the predictive variance that corresponds to sample variance while the aleatoric uncertainty is the term associated with the mean estimated variance of the data.

## 2.2. Network architecture

We use a U-Net [9] architecture modified as follows:

- We used two 3D convolutional layers, one at the start and one at the end. This improved sharpness and slice-to-slice consistency.
- We downsampled and upsampled three times instead of four. Experimental results showed no improvement with four downsample operations.
- We substituted max-pooling layers for strided convolutions in downsampling. For upsampling we used nearest-neighbor interpolation followed by a  $5^2$  convolution [11].
- We attached two heads to the end of the network, where one output  $\hat{\mathbf{y}}$  and the other output  $\hat{\sigma}^2$ . Both consisted of  $3^3$  and  $1^3$  convolutional layers.
- We concatenated the input image to the feature maps output by the network immediately before both heads [12].
- We used spatial dropout [13] ( $p = 0.2$ ) on all layers except the heads, because it drops weights on convolutional layers unlike standard dropout [7].

- We used the AdamW optimizer [14] with weight decay  $10^{-6}$ , learning rate 0.003,  $\beta = (0.9, 0.99)$ , and batch size 36.
- We used  $T = 50$  weight samples in prediction.

## 3. EXPERIMENTS

We conducted three experiments: 1) an experiment to validate that we capture both epistemic and aleatoric uncertainty, 2) an experiment translating CT to MR in the presence of anomalies to show that uncertainty is captured, as expected, in the anomalous region, and 3) a comparison of the synthesized  $T_1$ -w image created with the proposed method and the synthesized  $T_1$ -w image created with a traditional U-Net and MSE loss.

### 3.1. Dataset

We used non-contrast  $T_1$ -w and CT images from 51 subjects on a protocol for retrospective data analysis approved by the institutional review board. Fifty of the subjects were considered to be healthy and the remaining subject had anomalies in the brain and was excluded from training and validation. See Reinhold et al. [10] for additional dataset details. All  $T_1$ -w images were processed to normalize the white matter mean [15] and all images were resampled to have a digital resolution of  $0.7 \times 0.7 \times 1.0 \text{ mm}^3$ . Finally, the  $T_1$ -w images were rigidly registered to the CT images. For training, the  $T_1$ -w and CT images were split into overlapping  $128 \times 128 \times 8$  patches. Test images were split into three overlapping segments along the inferior-superior axis due to memory constraints.

### 3.2. Uncertainty validation on synthetic data

To show that we capture epistemic uncertainty, we trained four networks with 3, 5, 15, and 45 datasets. The remaining 5 healthy images are used for validation/testing. Each network is trained until the validation loss plateaued. In this experiment, we expect to see epistemic uncertainty decrease on the held-out in-sample data as the training data size increases. We see this in the left-hand plot of Fig. 1.

To show that we capture aleatoric uncertainty, we used the network trained on 45 datasets and added varying levels of zero-mean Gaussian noise to the test data (standard deviations of 10, 20, 30, 40, and 50). The right-hand plot in Fig. 1 shows the mean aleatoric uncertainty over the entire image and the brain mask. As expected, we see that aleatoric uncertainty increases with the level of noise. Aleatoric uncertainty over the whole image increases more slowly than inside the brain because, regardless of the noise level, the network predicts relatively low aleatoric uncertainty in the background.

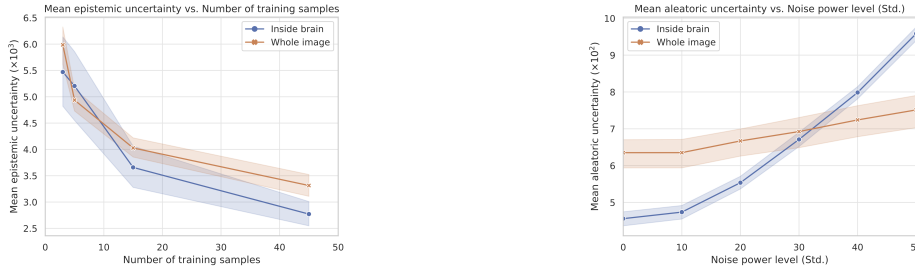


**Fig. 1. Uncertainty validation results:** Shown are the mean epistemic (left) and aleatoric (right) uncertainty. Shaded regions are bootstrapped 95% confidence intervals.

### 3.3. Anomaly localization

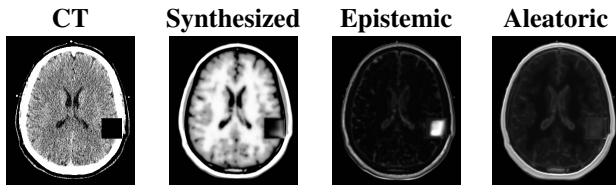
A DNN trained only on healthy data should exhibit high epistemic uncertainty for input containing pathologies or, more generally, anomalies. We quantitatively show this by inserting synthetic anomalies into the test data and measuring the relative epistemic uncertainty inside and outside the anomaly.

Our synthetic anomaly is an all-zero cube of side-length 40 voxels. This is placed randomly inside the brain mask of the five held-out healthy CT images (see Fig. 2 for an example). We create five of these anomalies per test subject by varying anomaly location, which results in a total of 25 anomalous test images. These synthetic anomalous data are used as input to the network trained on 15 datasets (described in Section 3.2). Figure 3 shows the mean epistemic uncertainty inside and outside the anomaly.

We also tested the model on the held-out pathological dataset collected on the same scanner. The results are shown in Fig. 4 with the generated epistemic and aleatoric uncertainties for the input CT image.

### 3.4. Comparison with U-Net

In this experiment, we compare the synthesis quality of our modified U-Net to a standard U-Net. To conduct this test, we used essentially the same network as previously described except 1) there is only one head associated with the synthesized  $T_1$ -w image, 2) we did not use any dropout, and 3) we used MSE as the loss function. We trained this U-Net and our proposed model on the same 45 healthy image pairs.



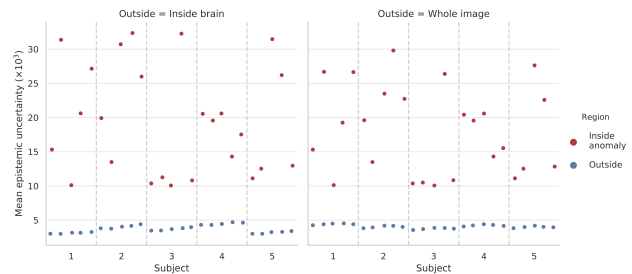
**Fig. 2. Synthetic anomaly:** Shown is an example synthetic anomaly CT image and the corresponding synthetic  $T_1$ -w image and estimated epistemic/aleatoric uncertainty.

Figure 4 shows a qualitative result where we examine the differences in synthesis quality on the held-out anomalous image. Both the U-Net and proposed method fail to correctly synthesize a portion of the brain in the occipital lobe due to the presence of an anomaly; however, the epistemic uncertainty map identifies that region as uncertain.

Various quantitative metrics on the five held-out datasets show worse performance on the proposed network as compared to the U-Net. This degraded performance disagrees with the results by Bragman et al. [3] who argue that the multi-task architecture regularizes training. We believe the cause of our degraded performance is due to: 1) the high noise levels associated with the input CT (in contrast, Bragman et al. explored MR-to-CT synthesis) and 2) that the proposed network—in spite of averaging multiple samples—has  $\sim 20\%$  fewer weights (in each pass) compared to the standard U-Net.

## 4. CONCLUSIONS

We have shown that epistemic and aleatoric uncertainty can be estimated in a medical image translation task with mod-



**Fig. 3. Epistemic uncertainty in synthetic anomaly:** Shown are the mean epistemic uncertainty inside the anomaly and outside the anomaly for the 25 test images. Outside is defined as the remainder of the brain mask (left-hand side) or the remainder of the image (right-hand side). Epistemic uncertainty inside the anomaly differs slightly between the two plots because the synthetic anomaly was sometimes partly outside the brain mask.

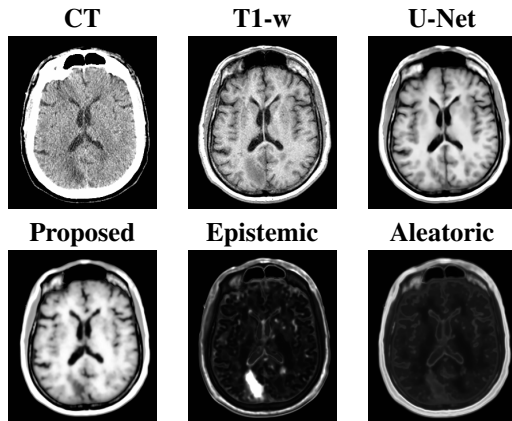


**Fig. 4. Example anomalous image:** Shown is an example anomalous image and corresponding synthesized images using both the standard U-Net (top row, far right) and the proposed method (bottom row, far left). The bottom row middle and right image show the proposed method’s additional outputs of estimated epistemic and aleatoric uncertainty maps.

ifications to a standard DNN. As shown in prior work (e.g., [3, 5]), the final experiment demonstrates how having an estimate of uncertainty adds insight into a quantitative result (see Fig. 4). The U-Net prediction provides no measure of uncertainty and estimates the structure of the anomalous brain incorrectly, which is not immediately obvious upon review of the synthetic image. The proposed network has a similar problem in the synthesized image; however, because the epistemic uncertainty is high in the anomalous region, we know not to trust the corresponding synthesized values. Likewise, the uncertainty in the skin and fat outside the skull has both high aleatoric and epistemic uncertainty which tells us that the model has difficulty estimating the values in those areas and that those synthesized regions cannot be trusted. Since we have shown that epistemic and aleatoric uncertainty is captured, as defined, in a medical image translation task, we can have more trust in these uncertainty estimates for downstream applications and analysis.

## 5. REFERENCES

- [1] C. Guo et al., “On calibration of modern neural networks,” in *Proceedings of the 34th International Conference on Machine Learning-Volume 70*. JMLR, 2017, pp. 1321–1330.
- [2] A. Der Kiureghian and O. Ditlevsen, “Aleatory or epistemic? does it matter?,” *Structural Safety*, vol. 31, no. 2, pp. 105–112, 2009.
- [3] F. Bragman et al., “Uncertainty in multitask learning: joint representations for probabilistic MR-only radiotherapy planning,” in *International Conference on Medical Image Computing and Computer-Assisted Intervention*. Springer, 2018, pp. 3–11.
- [4] T. Nair et al., “Exploring uncertainty measures in deep networks for multiple sclerosis lesion detection and segmentation,” in *International Conference on Medical Image Computing and Computer-Assisted Intervention*. Springer, 2018, pp. 655–663.
- [5] R. Tanno et al., “Uncertainty quantification in deep learning for safer neuroimage enhancement,” *arXiv preprint arXiv:1907.13418*, 2019.
- [6] Y. Gal and Z. Ghahramani, “Dropout as a bayesian approximation: Representing model uncertainty in deep learning,” in *International conference on machine learning*, 2016, pp. 1050–1059.
- [7] N. Srivastava et al., “Dropout: a simple way to prevent neural networks from overfitting,” *The Journal of Machine Learning Research*, vol. 15, no. 1, pp. 1929–1958, 2014.
- [8] A. Kendall and Y. Gal, “What uncertainties do we need in bayesian deep learning for computer vision?,” in *Advances in neural information processing systems*, 2017, pp. 5574–5584.
- [9] O. Ronneberger et al., “U-Net: Convolutional networks for biomedical image segmentation,” in *International Conference on Medical image computing and computer-assisted intervention*. Springer, 2015, pp. 234–241.
- [10] J. Reinhold et al., “Finding novelty with uncertainty,” in *Medical Imaging 2020: Image Processing*. International Society for Optics and Photonics, 2020.
- [11] A. Odena et al., “Deconvolution and checkerboard artifacts,” *Distill*, 2016.
- [12] C. Zhao et al., “Whole brain segmentation and labeling from CT using synthetic MR images,” in *International Workshop on Machine Learning in Medical Imaging*. Springer, 2017, pp. 291–298.
- [13] J. Tompson et al., “Efficient object localization using convolutional networks,” in *Proceedings of the IEEE Conference on Computer Vision and Pattern Recognition*, 2015, pp. 648–656.
- [14] I. Loshchilov and F. Hutter, “Decoupled weight decay regularization,” in *International Conference on Learning Representations*, 2019.
- [15] J. Reinhold et al., “Evaluating the impact of intensity normalization on MR image synthesis,” in *Medical Imaging 2019: Image Processing*. International Society for Optics and Photonics, 2019, vol. 10949, p. 109493H.